Organic and Carbon Aerogels from the NaOH-Catalyzed Polycondensation of Resorcinol–Furfural and Supercritical Drying in Ethanol

Dingcai Wu, Ruowen Fu, Zhiquan Yu

Materials Science Institute, Key Laboratory of Polymeric Composite and Functional Materials Laboratory, Zhongshan University, Guangzhou, 510275, People's Republic of China

Received 7 June 2004; accepted 8 October 2004
DOI 10.1002/app.21582
Published online in Wiley InterScience (www.interscience.wiley.com).

ABSTRACT: Organic aerogels and related carbon aerogels were prepared from the NaOH-catalyzed polycondensation of resorcinol–furfural (RF) and supercritical drying in ethanol. The effect of the preparation conditions, including the RF concentration, molar ratio of resorcinol (R) to NaOH, and molar ratio of R to furfural, on the gelation time and bulk density was studied. The chemical structure of the organic aerogel was revealed by IR spectroscopy. The pyrolysis process of the organic aerogel was investigated by thermogravimetric analysis. According to characterizations of transmission electron microscopy and nitrogen adsorption, the organic and carbon aerogels we obtained had a three-dimensional network that consisted of around 30-nm particles, which defined numerous mesopores of less than 30 nm. As a result, the aerogels had high Brunauer–Emmett–Teller surface areas (698–753 m^2/g) and large mesopore volumes (1.09–1.64 cm^3/g). X-ray diffraction characterization indicated that the carbon aerogel was more crystalline than activated carbon but less activated than graphite. © 2005 Wiley Periodicals, Inc. J Appl Polym Sci 96: 1429–1435, 2005

Key words: catalysts; gelation; pyrolysis; structure

INTRODUCTION

Organic and carbon aerogels are highly porous light materials possessing a number of exceptional and even unique physical properties that are of a noticeable interest for applications as varied as electric double-layer capacitors, thermal and phonic insulators, chromatographic packings, adsorbents, and catalyst supports.[1–4] Generally, carbon aerogels are obtained through the polycondensation of raw materials in an aqueous solution, solvent exchange, supercritical drying, and carbonization. This multistep procedure requires tedious preparation times and, thus, limits the commercial applications of the aerogels. Therefore, many other kinds of preparation methods have been subsequently developed to simplify the preparation process.[5–9] For example, Fu et al.[5] recently reported a new method for the preparation of carbon aerogels. In Fu et al.'s study, resorcinol (R) and furfural (F) were polymerized in isopropyl alcohol with HCl as a catalyst, and the resultant alcogels were then dried directly with supercritical isopropyl alcohol, which was followed by carbonization. This method eliminates the need for a solvent-exchange step before supercritical drying, so it is a simpler and easier process than the typical method of CO_2 supercritical drying widely used at present.[5] However, basic catalysts, as we know, are generally used in the fabrication of carbon aerogels because they have a better ability to achieve a high crosslink density than acid catalysts. In addition, the reaction of R and F is best induced by basic catalysts because F can self-condense under acid conditions to form a gel.[10] Therefore, the search for suitable basic catalysts for the system is important to further develop a new fabrication method. It regrettable that most inorganic catalysts widely used for the preparation for carbon aerogels are unable to carry out the sol–gel polymerization of R and F because of their low solubility in isopropyl alcohol.[5] For this reason, we previously chose to use an organic compound, that is, hexamethylenetetramine, as the catalyst for the gelation of resorcinol–furfural (RF) in isopropyl alcohol and successfully prepared carbon aerogels by this new method.[6] In this study, our goal was to find a normal inorganic base catalyst with acceptable solubility in other organic solvents and subsequently study the possibility of it inducing the sol–gel polymerization of

Correspondence to: R. Fu (cesfrw@zsulink.zsu.edu.cn).
Contract grant sponsor: Scientific Research Foundation for the Returned Overseas Chinese Scholars, State Education Ministry.
Contract grant sponsor: Specialized Research Fund for the Doctoral Program of Higher Education
Contract grant sponsor: Team Project of the Natural Science Foundation of Guangdong; Contract grant number: 20003038.

TABLE I
Effect of the Preparation Conditions on the Gelation Time and the Bulk Density

Test	R/NaOH	R/F	RF content (40 wt %)	Gelation time (h)	Density of AG (cm^3/g)		Density of CA (cm^3/g)
					Theoretical	Actual	
A1	50	1/2.5	10	No gelation	0.08		
A2	50	1/2.5	20	$102< t_g <130$	0.17	—[a]	—[a]
A3	50	1/2.5	30	36.5	0.26	0.26	0.33
A4	50	1/2.5	40	20.1	0.37	0.44	0.57
A5	50	1/2.5	50	13.4	0.48	—[b]	—[b]
A6	50	1/2.5	70	3.6	0.74	—[b]	—[b]
B1	25	1/2	40	5.2	0.37	0.61	0.77
B2	50	1/2	40	13.6	0.37	0.55	0.72
B3	100	1/2	40	30.0	0.37	0.55	0.66
B4	200	1/2	40	93.7	0.37	0.40	
B5	300	1/2	40	117.7	0.37	—[a]	—[a]
C1	50	1/1.5	40	10.6	0.37	0.68	0.82
C2	50	1/2	40	13.6	0.37	0.55	0.72
C3	50	1/2.5	40	20.1	0.37	0.44	0.57
C4	50	1/3	40	23.1	0.37	0.40	0.50

AG = organic aerogels; CA = carbon aerogels; t_g = glass-transition temperature. Reaction time = 7 days; reaction temperature = 80°C.
[a] The data were not measured because the strength of the RF alcogel was too weak to be dried.
[b] The data were not measured because the RF aerogels broke to pieces after supercritical E drying.

R and F in the organic solvent. As we know, NaOH has an exceptionally high solubility in methanol and ethanol (E; 0.24 g of NaOH/mL of methanol and 0.14 g of NaOH/mL of E, respectively[11]). Therefore, there are significant opportunities in the preparation of organic and carbon aerogels from the gelation of RF with this normal inorganic base catalyst and supercritical drying in methanol or E (in this study, E was selected as the representative solvent). In this study, such a synthetic route proved to be experimentally feasible. The preparation conditions, including the RF concentration, molar ratio of R to NaOH, and molar ratio of R to F, were tested in this study, and the texture and structure of the products prepared were characterized by means of IR, transmission electron microscopy (TEM), surface area analysis, thermogravimetric analysis (TGA), and X-ray diffraction (XRD).

EXPERIMENTAL

Sample preparation

Predetermined amounts of R, F, and NaOH were mixed in an appropriate amount of E at room temperature according to the predetermined recipes shown in Table I. The mixture was decanted into a glass vial (20-cm^3 capacity). We sealed the vial and then heated it to 80 ± 2°C in a water bath for 7 days. Subsequently, the organic gels were transferred into a pressure vessel and dried under E supercritical conditions (255°C, 12 MPa). Finally, the organic aerogels were carbonized with a quartz tube furnace at 900°C at a heating rate of 5°C/min for 3 h under a N_2 atmosphere (N_2 flow rate = 800 mL/min).

Characterization

We determined the bulk density of the aerogels by weighing the cylinder and dividing the weight by the measured geometrical volume.

The IR measurements of the RF aerogel are performed with IR spectroscopy (Bruker EQUINOX 55, Ettlingen, Germany) with the KBr disk method. The sample was well mixed with KBr and then sheeted.

The thermal characterization of the RF aerogel was determined by TGA (Netzsch TG 209, Bavaria, Germany). The samples were exposed to a high-purity nitrogen atmosphere at a heating rate of 100°C/min.

Some powders were scraped from the bulk carbon aerogel samples and dispersed with E onto a copper grid for microscopic examination. The structures of the carbon aerogel samples were observed with a JEM-2010H transmission electron microscope (JEOL, Tokyo, Japan).

Samples of approximately 0.1 g were evacuated at 150°C for the organic aerogels or at 250°C for the carbon aerogels before the adsorption measurements. It took about 10 h to guarantee that all of the adsorbed species were removed. Nitrogen adsorption and desorption isotherms were then taken with an ASAP 2010 surface area analyzer (Micromeritics Instrument Corp., Atlanta, GA). Equilibration interval and low-pressure dose were 10 s and 12 cm^3g^{-1}, respectively. It took more than 1 day to measure the N_2 adsorption–desorption isotherms of the samples. The Brunauer–Emmett–Teller surface area (S_{BET}), micropore size distribution, micropore volume (V_{mic}), micropore surface area (S_{mic}), mesopore size distribution, mesopore sur-

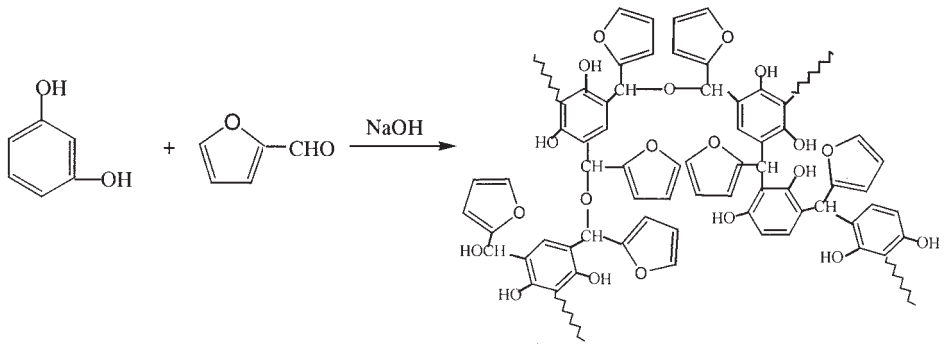

Figure 1 Schematic diagram of the reaction of R and F catalyzed by NaOH.

face area (S_{mes}), and mesopore volume (V_{mes}) of the samples were analyzed by Brunauer–Emmett–Teller theory, t-plot theory, Horvath–Kawazoe theory, and Barrett–Johner–Halendar (BJH) theory, respectively.

XRD patterns were collected with a D/max-IIA diffractometer (Rigaku Corp., Tokyo, Japan) equipped with a Cu Kα source.

RESULTS AND DISCUSSION

Gelation chemistry

Generally, as the polycondensation reaction proceeded, the RF solution changed from buff to yellow to reddish brown in color and, finally, slowly formed the dark RF alcogel. According to ref. 10, the higher aldehydes (e.g., F) react with phenol in much the same manner as formaldehyde, although at much lower rates. In addition, R undergoes all of the typical reactions of phenol but at a much faster reaction rate because of the enhanced election density in the 2, 4, and 6 ring positions.[12] Therefore, it seemed quite credible that R reacted with F through a reaction mechanism similar to the reaction of R and formaldehyde as described in detail in ref. 13. Like formaldehyde, F may have reacted with R with NaOH as a catalyst to form mixtures of addition and condensation compounds, which could have reacted further to form a crosslinking network. The principal reactions involved could have included (1) the formation of α-furfurylhydroxymethyl derivatives of R, (2) the condensation of the α-furfurylhydroxymethyl derivatives to form α-furfurylmethylene ether bridged compounds, and (3) the disproportionation of the α-furfurylmethylene and α-furfurylmethylene ether bridges to form α-furfurylmethylene bridges plus F as a byproduct. Figure 1 shows a schematic diagram of the fundamental reaction of R with F catalyzed by NaOH. For simplicity, we omitted the secondary reactions of R and F. For example, furan ring scission and the reaction with another R nucleus may have occurred, similar to the F–phenol reaction.[14]

These supposed principal reactions could be supported in part by the observation of the IR spectrum of the resultant organic aerogel (see Fig. 2). It was clear that due to the negative inductive ($-I$) effect of the furan group, the C—O—C stretching frequency shifted from its normal position of about 1222 and 1092 cm^{-1} to higher wave numbers (i.e., 1288, 1223, and 1173 cm^{-1}) as compared to R–formaldehyde aerogels,[13] which confirmed the presence of α-furfurylmethylene ether bridges between R molecules. The broad absorption band around 3457 cm^{-1} was characteristic of OH stretching vibrations. This strong, broad band had weaker shoulders at 2979 and 2929 cm^{-1}, which were attributed to aromatic, furan, and α-furfurylmethylene C—H stretching vibrations. IR absorption bands at 1616, 1500, 1470, and 1442 cm^{-1} were associated with aromatic and furan ring (C=C) stretching vibrations.[15] The band at 1016 cm^{-1} was associated with the furan 1030–1015-cm^{-1} band, and the bands at 794 and 737 cm^{-1} were assigned to aromatic and furan CH out-of-plane bending vibrations.[15] The spectrum in Figure 2 contains a band at 1707 cm^{-1}, which was theoretically not present in the spectrum of the resultant organic aerogels. We as-

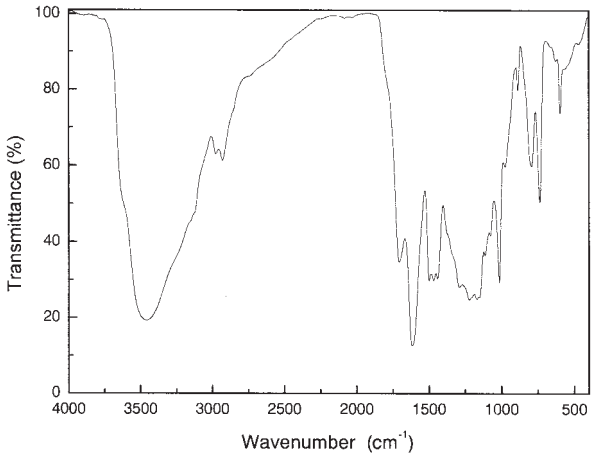

Figure 2 IR spectrum of the AG-A3 RF aerogel.

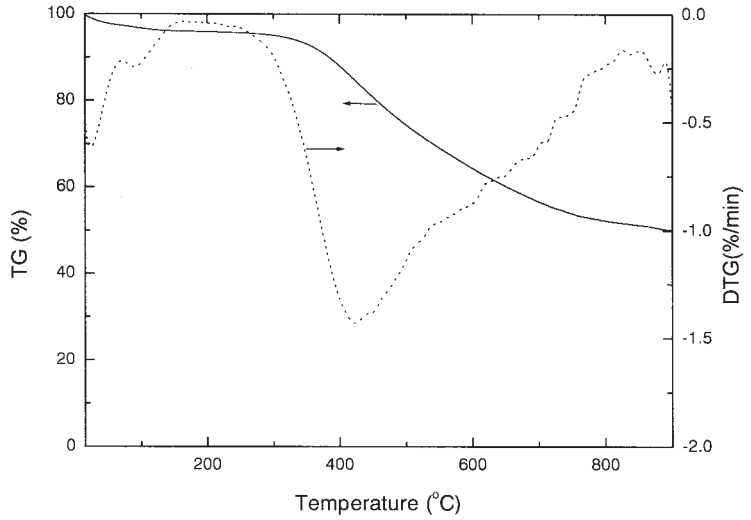

Figure 3 TG and dynamic thermogravimetry (DTG) curves taken during the pyrolysis of the AG-A3 RF aerogel.

signed it to the C═O stretching vibrations of the quinone derivates, which could have been from the oxidization of the Rs in the backbone due to the high-temperature treatment during the E supercritical drying process. However, this band could have also received contributions from the carbonyls formed on such secondary reactions as the furan ring scission and the reaction with the R nucleus. This indicated that the resultant organic aerogel could have had a more complicated structure.

The physical and chemical structures of the precursory organic gels were formed in the gelation process; because of this, the sol–gel process through the previously discussed principal reactions was the determinative steps during the preparation of the aerogels. For this reason, we investigated the effect of the preparation conditions on the gelation time (indicative of the gelation process), as shown in Table I. Here, the gelation time is the time interval between the introduction of the vial to the water bath and the gelation point (the moment when the surface of the sol no longer flowed in the vial tilted at an angle of 45° at 80°C), although it was somewhat arbitrary. As shown in Table I, the gelation rate experienced an exponential decrease with decreasing RF concentration. Although the gelation time was only a few short hours (3.6 h) when the RF concentration was 70 wt %, it was upward of 100 h when the RF concentration decreased to 20 wt %. In addition, the sol–gel transformation failed to occur under the conditions used in this study when the RF concentration was as low as 10 wt %, indicating that the RF content was one of the key factors determining whether the sol–gel polymerization could be carried out.

The experimental results of B1 to B4 in Table I shows the gelation time became shorter and shorter with decreasing R/NaOH, indicating that the increase in NaOH helped to accelerate the sol–gel reaction. However, the gelation time slightly increased with increasing R/F, as judged from the tests C1–C4.

These experimental results indicate that the sol–gel polymerization rate could be increased by decreasing the R/F ratio or by increasing RF concentration or NaOH content. On the basis of this conclusion, we could purposely make the sol–gel transformation occur anytime among a very wide gelation time range of about 3.6–130 h and thus tailor a series of aerogels with various physical and chemical structures to meet one's expectation, provided that suitable preparation conditions were selected.

Influence of the preparation conditions on the bulk density of the aerogels

Table I shows the effect of the major preparation conditions on the bulk density of the organic and carbon aerogels obtained in this study. As shown by the experimental results, we could control the bulk density of the organic aerogels and related carbon aerogels by changing RF concentration, NaOH content, or R/F ratio. Not surprisingly, the bulk density of the RF aerogels increased with increasing RF concentration, as shown by a comparison of the results of A3 and A4 in Table I.

When the R/NaOH ratio increased from 25 to 100, we found (see Table I) that the bulk densities of the RF aerogels almost remained unchanged but were all larger than the theoretic bulk density. When the R/NaOH ratio further increased to 200, the densities were very close to the theoretic bulk density, although the aging time (the time given by subtraction of the gelation time from the reaction time) was relatively short (because the gelation time was long). However, when the R/NaOH ratio was up to 300, the resultant

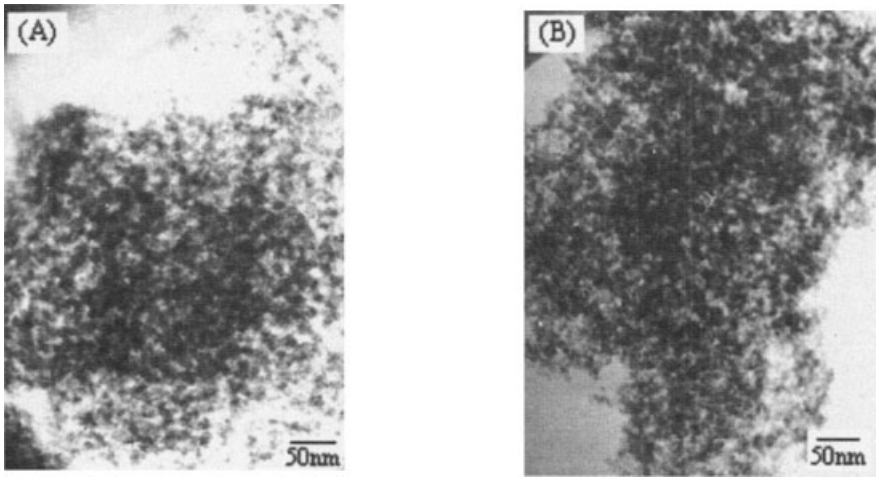

Figure 4 TEM photographs of typical prepared organic and carbon aerogel samples: (A) AG-A3 and (B) CA-A3.

RF aerogel was too weak in strength to be dried because the aging time was too short (see Table I). Generally, a decrease of the catalyst content (i.e., an increase in R/NaOH in this study) leads to a decrease of the initial nuclei in the polycondensation reaction and, thus, helps to increase the particle size of RF aerogels, consequently leading to a smaller drying shrinkage.[16–18] Thus, we suggest that a properly high R/NaOH ratio should be recommended to decrease drying shrinkage.

In addition, the results of the tests from C1 to C4 show that the bulk density of RF aerogels increased with increasing R/F, although the theoretic bulk density of all samples were the same. This may have been because the increase in F (i.e., the decrease in R/F) could enhance the crosslinking density during the sol–gel polycondensation of RF and then helped to obtain a smaller drying shrinkage.

Further, we concluded from Table I that the bulk density of carbon aerogels was bigger than that of their respective precursory RF aerogels and had the same preparation condition dependence as that of their respective precursory RF aerogels.

Carbonization process of the organic aerogels

Figure 3 shows the thermogravimetry (TG) and related TGA curves taken during pyrolysis of a typical RF organic aereogel. First, it is clear from Figure 3 that the organic aerogels obtained in this study had a steady structure before 300°C under an inert atmosphere. Further investigation showed that the pyrolysis of the organic aerogel could be divided into four stages. First, before 150°C, the mass loss was about 4% due to the physical desorption of residual solvent in the aerogel. Second, between 150 and 300°C, only about 1% mass loss occurred. Third, from 300 to 800°C, a large mass loss (ca. 43%) occurred, which was related to the release of small molecules such as H_2O, CO, and CO_2, indicating that the aerogel framework began to collapse and formed an extended, interconnected carbon structure.[19] Fourth, above 900°C, a small 2% weight loss was observed, which was attributed to the elimination of organic residues in gaseous form, which slowly diffused out of the pores.[19]

Morphology of the organic and carbon aerogels

TEM observations [see Fig. 4(A)] showed that the organic aerogels prepared in this study had an interconnected bead structure analogous to that of the typical aerogels prepared by Pekala.[13] These beads were generally about 10 nm; and the pore size was smaller than 40 nm. In addition, there was no apparent difference

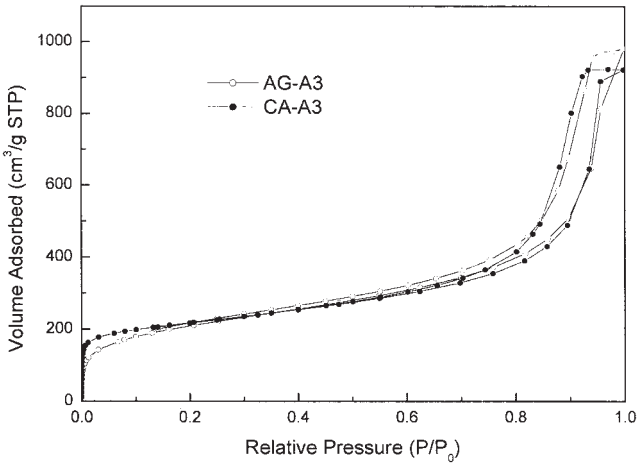

Figure 5 N_2 adsorption–desorption isotherms of the representative prepared organic and carbon aerogel samples. STP = standard temperature and pressure; P/P_0 = the ratio of the adsorption pressure (P) and the saturation vapor pressure (P_0).

TABLE II
Textual Characteristics of the Representative Samples in the Study

Sample	S_{BET} (m^2/g)	S_{mic} (m^2/g)	S_{mes} (m^2/g)	V_{mic} (cm^3/g)	V_{mes} (cm^3/g)
AG-A3	753	94	639	0.03	1.49
CA-A3	752	326	511	0.15	1.33
AG-A4	719	101	698	0.04	1.64
CA-C4	698	304	528	0.14	1.09

in the texture between the RF aerogel and its related carbon aerogel, as judged from a comparison of Figures 4(A) and 4(B).

Porous structure of the organic and carbon aerogels

Figure 5 shows the nitrogen adsorption isotherms of the typical organic and carbon aerogel. According to the IUPAC classification,[20] the isotherms of the aerogels were type IV and had a hysteresis loop of type H2. According to the isotherms of the samples, the surface area, pore volume, and pore size of the samples were calculated, and the results are shown in Table II and Figure 6. The data in Table II reveal that the aerogels had high S_{BET} values (698–753 m^2/g) and large V_{mes} values (1.09–1.64 cm^3/g). Further investigation showed that carbonization helped the formation of micropores but seemed to impair the mesoporous structure, most likely due to the collapse of the network as the aerogel was exposed to elevated temperatures under a N_2 atmosphere (see Fig. 3). In addition, the average pore diameter of the typical organic and carbon aerogel was less than 40 nm (see Fig. 6), which was consistent with the results from the TEM observations shown in Figure 4.

Crystal structure of the carbon aerogel

To elucidate the structural appearance of the prepared carbon aerogel, XRD characterization was carried out, as shown in Figure 7. By comparing the XRD pattern in Figure 7 with those from three types of carbon materials (i.e., activated carbon, graphite, and a R–formaldehyde based carbon xerogel) reported in ref. 21, we could see that like the R–formaldehyde based carbon xerogel, the carbon aerogel obtained in this study possessed a broad peak at $2\theta = 23°$ related to the peaks for activated carbon and graphite and a small broad peak at $2\theta = 43°$, apparently associated to the peak for graphite. On the basis of this fact, we believe that the carbon aerogel prepared in this study was not completely amorphous and that it was more crystalline than activated carbon but less activated than graphite.[21]

CONCLUSIONS

NaOH was found to be a proper inorganic base catalyst for the sol–gel polymerization of R and F in E. On the basis of this fact, we successfully fabricated organic aerogels and related carbon aerogels by gelation and supercritical drying in E. The experimental results

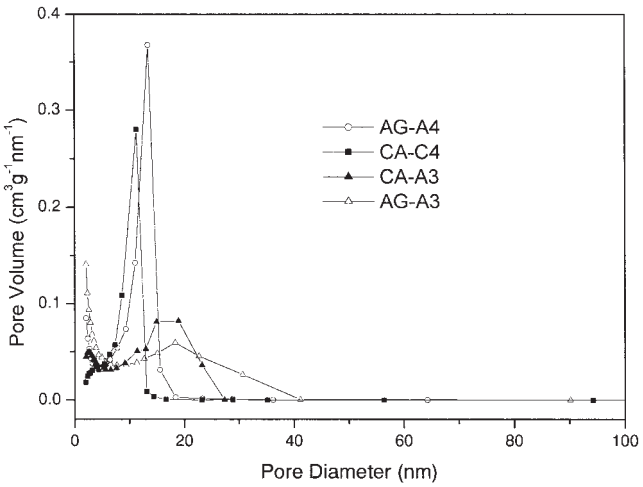

Figure 6 BJH pore size distribution of representative prepared aerogel samples.

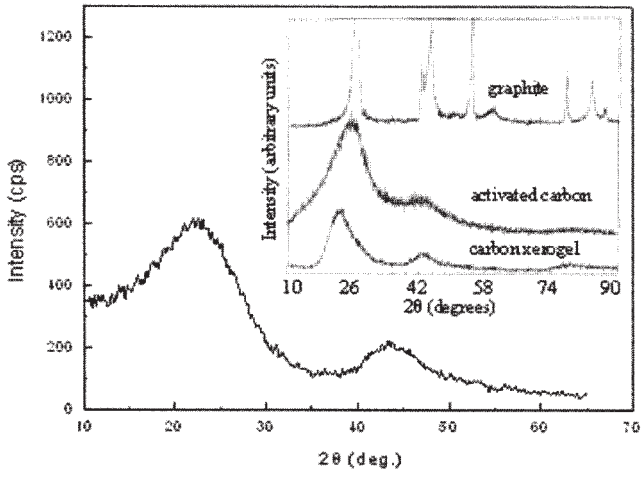

Figure 7 Comparison of the XRD pattern from a typical carbon aerogel obtained in this study (CA-A3) with those from three types of carbon materials (shown in the inset).

show that the sol–gel polymerization rate could be increased by a decrease in the R/F ratio or an increase in the RF concentration or NaOH content. In addition, the bulk density of the organic aerogels and related carbon aerogels could be controlled by these preparation conditions. The decrease in RF concentration, increase in R/F, and increase in R/NaOH all helped to decrease the bulk density of the aerogels. The framework of the aerogel samples consisted of interconnected nanoparticles about 20 nm in diameter, which defined numerous mesopores of less than 30 nm. As a result, the aerogels exhibited high S_{BET} values (698–753 m^2/g) and large V_{mes} values (1.09–1.64 cm^3/g). The pyrolysis process of the organic aerogel could be divided into four stages. The carbon aerogels possessed a partially nanocrystalline structure between activated carbon and graphite.

References

1. Mayer, S. T.; Pekala, R. W.; Kaschmitter, J. L. J Electrochem Soc 1993, 140, 446.
2. Pekala, R. W. U.S. Pat. 4,997,804 (1991).
3. Pajonk, G. M. Appl Catal 1991, 72, 217.
4. Hanzawa, Y.; Kaneko, K.; Yoshizawa, N.; Pekala, R. W.; Dresselhaus, M. S. Adsorption 1998, 4, 187.
5. Fu, R.; Zheng, B.; Liu, J.; Dresselhaus, M. S.; Dresselhaus, G.; Satcher, J.; Baumann, T. Adv Funct Mater 2003, 13, 558.
6. Wu, D.; Fu, R.; Zhang, S.; Dresselhaus, M. S.; Dresselhaus, G. J Non-Cryst Solids 2004, 336, 26.
7. Liang, C.; Sha, G.; Guo, S. J Non-Cryst Solids 2000, 271, 167.
8. Albert, D. F.; Andrews, G. R.; Mendenhall, R. S.; Bruno, J. W. J Non-Cryst Solids 2001, 296, 1.
9. Mayer, S. T.; James, L.; Pekala, R. W. U.S. Pat. 5,420,168 (1995).
10. Kopf, P. W. In Encyclopedia of Polymer Science and Technology; Mark, H. F.; Bikales, N. M.; Overberger, C. G.; Menges, G.; Kroschwite J. I., Eds.; Wiley: New York; Vol. 11, p 49.
11. Handbook of Reagents; Shanghai Chemical Reagent Co., Ed.; Shanghai Science: Shanghai, 2002; p 1186 (in Chinese).
12. Varagnat, J. In Encyclopedia of Chemical Technology; Mark, H. F.; Othmer, D. F.; Overberger, C. G.; Serborg G. T., Eds.; Wiley: New York, 1981; Vol. 13, p 39.
13. Pekala, R. W. J Mater Sci 1989, 24, 3221.
14. Knop, A.; Pilato, L. A. Phenolic Resins—Chemistry, Applications and Performance, Future Directions; Springer: Berlin, 1985; p 20.
15. Nakanishi, K.; Solomon, P. H. Infrared Adsorption Spectroscopy, 2nd ed.; Holden-Day: San Francisco, 1977; pp 19–21 and 47.
16. Bock, V.; Emmerling, A.; Saliger, R.; Fricke, J. J Porous Mater 1997, 4, 287.
17. Ruben, G. C.; Pekala, R. W.; Tillotson, T. M.; Hrubesh, L. W. J Mater Sci 1992, 27, 4341.
18. Tamon, H.; Ishizaka, H.; Mikami, M.; Okazaki, M. Carbon 1997, 35, 791.
19. Biesmans, G.; Mertens, A.; Duffours, L.; Woignier, T.; Phalippou J. J Non-Cryst Solid 1998, 225, 64.
20. Sing, K. S. W.; Everett, D. H.; Haul, R. A. W.; Moscou, L.; Pierotti, R. A.; Rouquerol, J.; Siemieniewska, T. Pure Appl Chem 1985, 57, 603.
21. Lin, C.; Ritter, J. A. Carbon 1997, 35, 1271.